Journal of Mines, Metals and Fuels, *73(5): 1203-1216; 2025. DOI: 10.18311/jmmf/2025/48215*

Print ISSN : 0022-2755

Journal of Mines, Metals and Fuels

Contents available at: *www.informaticsjournals.co.in/index.php/jmmf*

SGO-Based Optimized Lstm for Performing Vibration Analysis to Predict Fault in High-Speed Rail Tracks

Sanket G. Pandit[1,2]* and Laxman Yadu Waghmode[3]

[1]*Department of Space Engineering, School of Engineering, Ajeenkya DY Patil University, DY Patil Knowledge City, Pune – 412105, Maharashtra, India; sanketpandit642@gmail.com*

[2]*Shivaji University, Kolhapur - 416004, Maharashtra, India*

[3]*Department of Mechanical Engineering, Annasaheb Dange College of Engineering and Technology, Ashta – 416301, Maharashtra, India*

Abstract

Train bogies are vital components of trains since they are in close contact with the rails and support the weight of the train. Train bogie vibrations are dynamic loads caused by a variety of processes, including wheel and rail unevenness, impact at rail joints, and wheel flatness. In the frequency range of 1–80Hz, vibration is created which causes fault and uncomfortable for passengers. Numerous methods were introduced to predict the fault based on vibrations or some other signals. Yet those models are poor due to improper training, complex design, and poor fit for real-time utilization. To overcome these issues optimized LSTM combined with an auto encoder approach is developed to predict fault based on mechanical vibration in an effective way. Acoustic sensors are attached to a train bogie to capture the vibrations from the passing trains. After that, the encoder and decoder are the two main parts of the auto encoder, which is regarded as an unsupervised learning technique that denoises the original signal vibration. Finally, an optimized LSTM classifier is employed to classify fault and no-fault railway tracks in the pre-signals. Through the application of SGO optimization, which appropriately selected the learning rate and hidden neurons of LSTM, the performance of LSTM was enhanced. The suggested approach's effectiveness is evaluated utilizing performance metrics including specificity, recall, accuracy, and precision; the findings reveal 94.2 %, 92.5 %, 94.2 %, and 95 %. This analysis demonstrate that the suggested approach can anticipate a track's defect with accuracy using vibration data in a real-time scenario.

Major Findings: *The optimized LSTM combined with an autoencoder effectively predicts faults in train bogies based on mechanical vibrations, addressing issues from previous methods. Acoustic sensors capture train vibrations, and the autoencoder denoises the signal, enhancing fault detection accuracy.*

Keywords: *Autoencoder, Fault Detection, High-Speed Rail Tracks, Mechanical Vibration, Optimized Lstm Classifier, SGO Optimization*

1.0 Introduction

A train is an arrangement of linked automobiles used to carry passengers or cargo down a railroad track[1]. Though some trains, like multiple units, are self-propelled, locomotives or railcars, commonly simply referred to as engines, are usually responsible for pulling or pushing trains. Wagons, or railroad cars, are used to transport both passengers and goods[2]. Because trains use less fuel and produce fewer greenhouse emissions than other forms of land transportation, governments, environmentalists, and rail enthusiasts have advocated for increased rail usage since the 1970s[3]. The effects of railway traffic on the environment, such as vibration, noise, and pollution, are

*Author for correspondence

especially critical given the increased speed of the trains. With regard to railroad trains, such as France's T.G.V. (high-speed), this speed increase is extremely desirable[4]. In terms of vibration, this speed's impact is directly related to where it is about waves that are traveling through the earth. Two rails connected by rail pads and positioned on sleepers make up a track. The rail acts as a point of contact between the track and the train wheel. These identical components are strained by train vibrations that travel from the track through the ballast and the sleepers. There are multiple causes causing the vibrations caused by the dynamic stresses, including uneven wheels and rails, impact at the rail joints, and flat wheels. The frequency range in which mechanical vibration is perceived is 1 to 80 Hz, whereas ground-borne vibrations can produce noise in a structure between 16 and 200 Hz due to vibrations in secondary parts of a structure[5]. Over the past three decades, a substantial amount of study has been done to create rigorous analytical-numerical techniques and empirical tools for modelling countermeasures and predicting vibration caused by railway traffic under various loading situations. For the most part, an infinitely long periodic structure with modal behaviors and wave propagation properties can be represented by a train track[6-7]. Calculating a railroad track's reaction to a moving harmonic load as an endlessly long periodic structure is a crucial step in understanding track dynamics.

Numerous writers have conducted experimental studies that identify planetary gear defects by combining vibration extraction and machine learning methods. A few common machine learning methods, involving SVM (Support Vector Machines), Multilayer Perception Networks (MLP), and Artificial Neural Networks (ANN), were used to identify vibrations in the train system[8-11]. These models do, however, have drawbacks, including the possibility of bias, poor interpretability, issues with data privacy, high implementation costs and complexity, and a dependence on high-quality data. To tackle these issues, nowadays deep learning is mostly preferred for vibration prediction. The three primary advantages of using deep learning are shorter training times, improved neural network performance, and fewer data requirements. Based on these advantage, an optimized LSTM is used in the proposed model to predict the vibration in a train. The optimized LSTM was well-suited for processing sequences of data with long-range dependencies[12]. The main contribution of the proposed model is listed below,

- Optimized LSTM with an autoencoder framework is developed to analyze faults in railway tracks from vibration signals.
- The Autoencoder denoising technique is used for reducing noise in gathered vibration signals.
- Optimized LSTM is chosen for detecting faults in a train based on pre-vibration signal data.
- SGO optimization is utilized to improve the prediction performance by choosing the optimal value of the learning rate and hidden neurons.
- Performance of the suggested model was evaluated using some metrics such as recall, specificity, precision, as well as accuracy, and also the observed values were compared with some other traditional models.

The remainder of the paper is structured in this manner. The relevant literature on signal-based vibration detections is briefly reviewed in the following part, and Section 3 provides an explanation of the proposed methods. Section 4 shows the experimental results of the suggested model, and Section 5 presents the research's overall conclusion.

2.0 Literature Review

Numerous approaches have been developed to forecast mechanical vibrations. The following were some of the recently introduced ones that were discussed.

Cao *et al.* investigated the characteristics and mode of propagation of vibrations in the ground brought on by a high-speed train crossing the viaduct[13]. A field experiment was conducted, as well as the information gathered was thoroughly reviewed. The energy distribution properties of ground vibrations were investigated by applying a CWT (Continuous Wavelet Transform) to the vibration signal using time-frequency synchronization. Vibration response and frequency are continuously correlated before 4 Hz and after 16 Hz at different train speeds; however, train speed clearly influences ground vibration between 4 Hz and 16 Hz. Although more than 50 Hz dissipates a little bit from the top of the pier to the beam bottom due to the beam's high energy consumption[14,15].

Wu, *et al.* created a method to investigate the properties of vibration transmission in buildings through

wave propagation analysis, which clarifies the theory of building vibration transmission. The building's pattern was similar for each story, so it was initially modelled as a periodic structure[16]. The periodic structure model was developed on the basis of the wave propagation approach, allowing the spectral element method to be used to generate the cell structure's dynamic stiffness matrix[17].

Qin *et al.* developed an enhanced federated learning approach that uses Secure Boost in modelling to train local diagnosis models while lowering computing costs using wavelet packet decomposition. The suggested method It depends on the notion of protecting the privacy and confidentiality of bogie data and aims to build a global model of diagnosing bogie defects by merging model parameters of multiple railways in each iteration. However, the models include drawbacks such as inadequate data characteristics, which results in a poor ability of the model to generalize[18].

Liu *et al.* created a Conditional Generative Adversarial Network (CGAN), to solve the issue of unbalancing. This network creates synthetic samples that correlate to particular fault labels that fall under the minority groups. The models yield features that are described by the knowledge graph and the feature importance sequence list. However, it is challenging to obtain the desired modelling performance due to the issue of an imbalanced fault sample[19].

Sun *et al.* developed an IDRN (Improved Deep Residual Network) for diagnosing faults in trains. Initially, an innovative RCB (Residual Convolution Block) is suggested to enhance the hidden feature extraction process. Second, The residual block incorporates the Squeeze & Excitation block (SE) to enhance the sensitivity of the model to features. In the end, In order to accelerate IDRN's convergence, Adan is chosen as the optimizer. This model has the drawbacks of low diagnosis accuracy, sluggish diagnosis speed, and poor feature extraction capacity[20].

The above literature has a number of methods introduced to predict the train bogie vibration. Although these methods yield good results, they have several drawbacks, such as not providing the phase information of the signal under analysis[20], loss of signal amplitude, time-consuming and complicated designing, increase in noise and vibration, and needs to improve accuracy[21]. Those impacts are overwhelmed through the proposed optimized LSTM with autoencoder which detects the fault from the vibration signals. The working process of the proposed model is discussed below[22].

3.0 Proposed Method for Detecting Track Fault Due to Vibration

A train bogie is a trolley or wagon with wheels. A bogie is, mechanically speaking, a framework or chassis with wheels that is fastened to a rail vehicle and functions as a modular subassembly of axles and wheels. Train bogies vibrate as waves through the train and into the free field, originating at the wheel interface. Train vibration results in a number of issues that impact the High-Speed Train's (HST) vital speed, riding comfort, and safety. In this proposed model optimized LSTM is employed to effectively predict fault based on vibration. Figure 1 illustrates the process flow of the proposed model.

Initially, the data is collected from sensors which are linked to train bogie. The train bogie bearing-equipped structure is situated beneath a railroad car to which axles are connected. Autoencoder models are utilized to pre-process the gathered data by learning to recreate the original data from the noise signal. The pre-signals are provided in optimized LSTM to predict the vibration that is having in the train. The prediction performance of LSTM is improved through the use of shell game optimization which selects the optimal parameters like learning rate and hidden neurons based on the objective

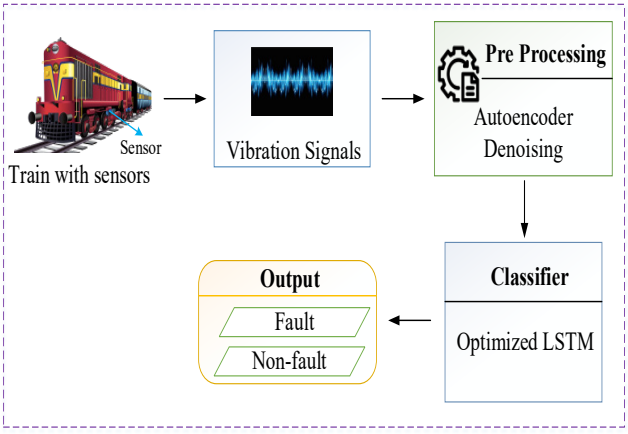


Figure 1. Architecture of rail vibration defect detection.

function. The modelling of each model is provided below.

3.1 Pre-Processing

The procedure for identifying and eliminating erroneous or corrupt records from a dataset is known as pre-processing. In the proposed model autoencoder-based pre-processing technique is employed to remove the noise signals from the vibrations. Unsupervised learning of data representations or encodings is made possible by a particular kind of neural network called auto encoders denoising. Reconstructing the original, noise-corrupted version of the input signal is their main goal. An autoencoder consists of two main components:

- Encoder: The partial information, z, is obtained by the encoder. The following is the non-linear transformation.

$$z = f(w\tilde{x} + b) \quad (1)$$

- Decoder: Z is transformed back into reconstructed data (x̂) by the decoder. The following is the nonlinear transformation:

$$\hat{x} = g(W'z + b') \quad (2)$$

Within the pre-processing function, the function f represents the input x̂ in a parameterized form with weight and bias parameters W and b. The parameters of the decoder are,W-'.and,b-'. The deep learning models employ non-linear activation functions, denoted as f and g. The overall parameter set that defines the non-linear parameterized equations of the encoder and the decoder is Ø= {W, b, W', b'}where θ = {W, b} represents the weight and bias matrix of the encoder as well as θ' = {W', b'} represents the weight and bias matrix of the decoder. By minimizing the reconstruction error—that is, the error between x and x̂ these parameters are optimized. The DAE's average reconstruction error looks like this:

$$\theta^*, \theta'^* = arg_{\theta,\theta'}\, min\, E_{q^\circ(x,\tilde{x})}[L_H\left(X_{,g\theta'}\left(f_\theta(\hat{X})\right)\right)$$

$$\left(X_{,g\theta'}(f_\theta(X))\right)] \quad (3)$$

Where $Ep_{(X)}$ [f(X)] when X has a probability density (X), X is the random variable that is associated with x for the expectation of f(x). As explained in the average reconstruction function of the basic autoencoder, the average reconstruction function of the autoencoder goes through a series of modifications to achieve the above form.

$$\theta^*, \theta'^* = arg_{\theta,\theta'}\, min\, \frac{1}{n} \sum_{i=n}^{n} L(x^{(i)}, g_{\theta'}(f_\theta(x^{(i)}))) \quad (4)$$

Where L is the loss function described as L(x, x̂)= ‖ x - x̂ ‖^2 and then the quantity of training samples is n. In a different method, the conventional loss function is swapped out for a Bernoulli distance loss function, which may be quantified using the reconstruction cross-entropy that follows:

$$L_H(x, \hat{x}) = (\beta_x || \beta_{\hat{x}} \quad (5)$$

Where β shows that the log-likelihood function is negative L_H (x, x̂) follows the distribution of Bernoulli. When L(x, x̂) is replaced L_H (x, x̂), the reconstruction function becomes

$$\theta^*, \theta'^* = arg_{\theta,\theta'}\, min\, E_{q^\circ(x)}[L_H\left(X_{,g\theta'}(f_\theta(X))\right)] \quad (6)$$

Where the empirical distribution related to the input is q^θ (x) is replaced by q^θ (x, x̂) a joint distribution as a result of random mapping. The fundamental idea behind an auto encoder is that z is the outcome of a stochastic mapping of x, not x itself, but rather a deterministic function of x̂. As a result, we obtain as an objective function that stochastic gradient descent minimizes.

3.2 Optimized LSTM Classifier

The operating safety of high speed trains is directly impacted by the condition of the bearing, which is a crucial part of the bogies. Therefore, it's imperative to identify bearing problems in high-speed train bogies as soon as feasible. As a result, the suggested study used an optimized LSTM to forecast the defect based on the pre-signal.

3.2.1 Working Process of LSTM

The problem of long-term dependencies in sequence prediction applications led to the development of RNNs (Recurrent Neural Networks) with LSTM (Long Short-Term Memory) architecture. It was introduced by

Hochreiter and Schmidhuber in 1997. By default, the LSTM classifier retains data information for an extended duration. In this case, it has already been demonstrated that the LSTM classifier is the best neural network option. Typically, the temporal quasi-periodic characteristics needed to extract the long- and short-term dependencies are kept in a sequence of LSTM units, which make up the LSTM classifier. Figure 2 illustrates the LSTM classifier's structure:

In the proposed model, the input is considered as pre-signals, and the output is considered as fault or non-fault. Equations are utilized to represent the input values of gate i_n, forget gate f_n cell c_n and output gate o_n of each individual LSTM unit.

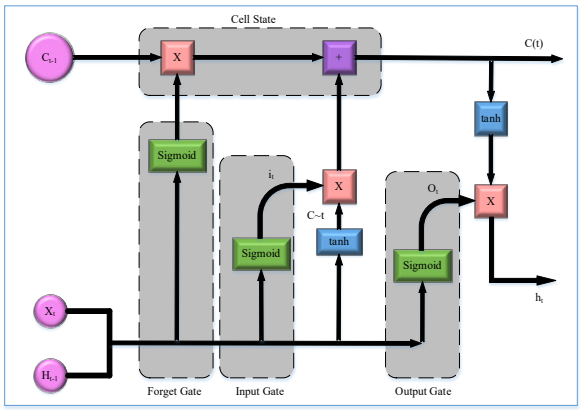


Figure 2. LSTM cell architecture.

$$i_n = \sigma(W_{ih}h_{n-1} + W_{ia}a_t + b_i) \quad (7)$$

$$f_n = \sigma(W_{fh}h_{n-1} + W_{fa}a_t + b_f) \quad (8)$$

$$c_n = f_n \times c_{n-1} + i_n \times \tan h(W_{ch}h_{n-1} + W_{ca}a_n + b_c \quad (9)$$

$$o_n = \sigma(W_{oh}h_{n-1} + W_{oa}a_n + b_0) \quad (10)$$

Where denotes the quasi-periodic characteristic at each of the n time steps in various frequency bands. h_(n-1) Is the output of the previous LSTM unit. W And b represent processing, and tanh(.) and σ(.) stand for the sigmoid & hyperbolic tangent activation functions, correspondingly. The following equation serves as a mathematical representation of the LSTM unit's output:

$$h_n = o_n \times \tan h(c_n) \quad (11)$$

The information from the previous time steps via c_n and o_n is collected in the LSM unit's output at time step n, , which also contains the extracted features. The cell state $\{c_n | n = 1, 2, , N\}$ learns memory information of the temporal quasi-periodic characteristics for short as well as long times based on the dependence relation during the training phase.

Before going on to the next section, it is important to discuss a major problem with neural networks. This problem is known as overfitting, and it is the ability of the network to match the training data but not the testing data since it has not been trained to generalize to new scenarios. When in an overfitting state, the neural network cannot perform to its full capacity; this may be the case with the LSTM scenario. One way to train the neural networks and avoid gradient explosion and disappearance is to use early halting operation with dropout and a weight limitation. During each iteration, Dropout randomly selects a subset of LSTM units and sets their output to zero. A portion of the remaining LSTM units are deleted and are only used when error backpropagation calculations are necessary. The error value is calculated using the output value of a small number of LSTM units. And it has an overfitting problem, to reduce with LSTM and hyper-parameters to optimized tune by using SGO optimization.

3.2.2 Shell Game Optimization (SGO)

In this game, participants attempt to uncover a ball buried beneath one of the three Shells. A little ball and three shells are provided by the operator in the classic game known as "the shell game"[15]. This game stimulates players' curiosity, which helps to improve their accuracy. First, this game makes players more curious, which enhances accuracy. Afterward, place the ball beneath a shell. The operator works with the shells on the table with their hands. The player is now asked by the operator to estimate which shell the ball is hidden beneath. Each player might select the right or incorrect shell based on their level of intelligence as well as precision. The player who correctly identifies the shell receives extra points.

The SGO procedure for choosing the ideal hidden neuron and learning rate parameters for the LSTM is shown below.

STEP 1: Initialization

At first number of persons n and their position in the shell game is initialized in the proposed model learning rate (L) and hidden neurons (H) are initialized

$$H = \{h_1, h_2, h_3 \ldots \ldots . h_n\} \quad (14)$$

$$L = \{l_1, l_2, l_3 \ldots \ldots . l_n\} \quad (15)$$

Where n number of optimization

STEP 2: Fitness Function

A specific kind of objective function known as a fitness function is used to summarise, in a single Figure of merit, the degree to which a given design solution approaches the predetermined goals.

$$RMS \sqrt{\frac{1}{n}\sum_i x_i^2} \quad (16)$$

Where a root mean square of the fitness function is RMS and the number of measurements is n and x_i is an each value.

STEP 3: Updating

Updating each solution to select the optimal value of the initialized parameter. Each population member's location is updated here to choose the best value, which is indicated as follows,

(17)

Where is a arbitrary value within the range of [0 1] $dx^d_{i,ball}$, $dx^d_{i,shell_2}$, $dx^d_{i,shell_3}$ are the shifts in dimensions 'd' of participant 'i' according to $shell_1$, $shell_2$ and $shell_3$.

STEP 3: Termination

It is the final procedure, once the optimal value is selected the overall process goes to the end, otherwise, the process continues from the computing fitness function. In the upcoming part, the performance of the proposed model was validated.

4.0 Result and Discussion

SGO-based LSTM with autoencoder denoising is formed to detect the fault from the mechanical vibration of the train. To acquire mechanical vibration data from the train by using the sensor. The collected data will be pre-processed using an autoencoder denoising to decrease vibration and noise. Afterward, detect the vibration level from pre-processed signal data using the optimised LSTM method. Python is used to analyze the performance of the suggested model on an Intel Core i7 CPU, NVIDIA GeForce RTX 3070 GPU, as well as 64GB RAM.

4.1 Dataset Description

This dataset focuses on the use of vibration detection on railway lines as a preventative maintenance technique[16]. Railway tracks are susceptible to defects due to trains constantly moving along them. These track flaws raise vibration frequencies on the track, and if they are not fixed, they will result in disastrous failures. Track frequencies are detected by vibration sensors; the greater the frequencies, the worse the track condition is. After that, data is extracted from the sensor and examined. If the analysis reveals frequencies higher than the threshold, prompt action is performed. The concepts of system engineering and maintenance are applied when installing the vibration sensors on the rail; the same principles

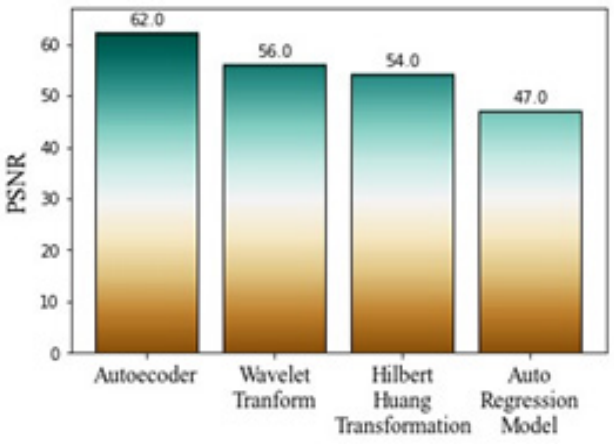


Figure 3. Comparison of the suggested PSNR and the current approach.

are also applied when operating the sensors. Using this dataset to predict the fault in a train, at first, the vibration signals are denoising using autoencoder. The working process of the autoencoder was validated using the following metrics.

Table 1. PSNR Values

Method	PSNR Value
Autoencoder	62.0
Wavelet Transform	56.0
Hilbert Huang Transformation	54.0
Auto Regression Model	47.0

Peak-Signal-To-Noise-Ratio (PSNR) comparison is shown in Figure 3. The ratio of a signal's highest possible strengths is called PSNR in engineering. Table 1 presents the PSNR values for different methods, demonstrating that the Auto encoder achieved the highest PSNR value of 62.0, followed by the Wavelet Transform at 56.0.The PSNR value of the auto encoder is 62 %, whereas the PSNR values of Wavelet Transform, Hilbert Huang Transformation, and Auto Regression model are 56%, 54%, and 47%, respectively. This proves the proposed model has a higher PSNR value than the present approaches.

Table 2. SNR Values

Method	SNR Value
Autoencoder	56.0
Wavelet Transform	53.0
Hilbert Huang Transformation	48.0
Auto Regression Model	45.0

As shown in Table 2, the SNR values indicate that the Autoencoder performs best with an SNR value of 56.0, while the Auto Regression Model has the lowest value of 45.0.The SNR (Signal-to-Noise Ratio) comparison, which contrasts the strength of a desired signal with the level of background noise, is depicted in Figure 4. The autoencoder has an SNR value is 56 %, whereas the SNR value of existing techniques like Wavelet Transform, Hilbert Huang Transformation, and Auto Regression model are 53 %, 48 %, and 45 % respectively. This proves the proposed model has a higher SNR value than the present approaches.

The bit error rate, or BER, is a measure that shows how frequently an error requires the retransmission of a packet or other data unit. Comparison of BER is illustrated in Figure 5, thus showing the autoencoder has 0.1% BER which was lower than that of the other methods like

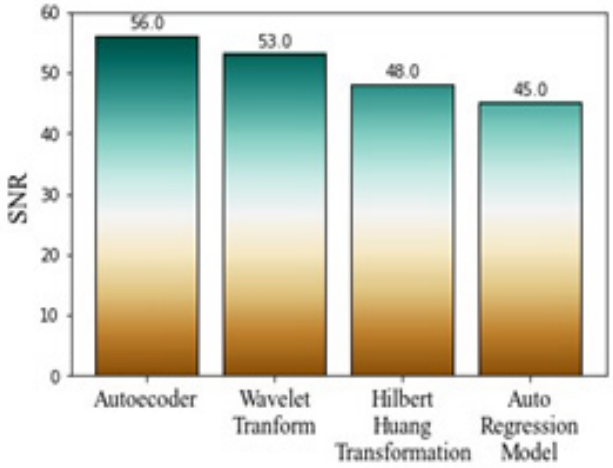


Figure 4. Comparison of SNR.

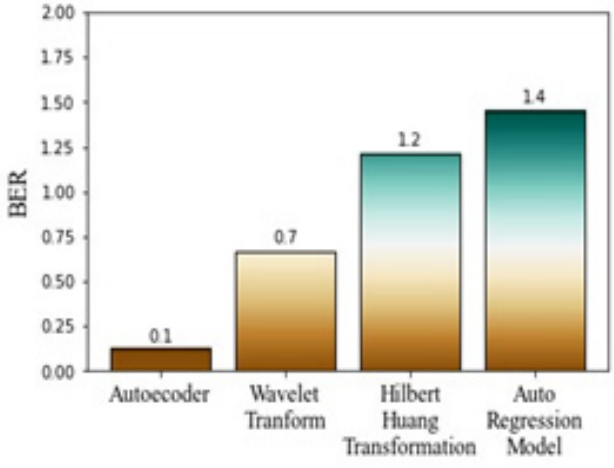


Figure 5. Comparison of BER proposed and existing method.

Table 3. BER Values

Method	BER Value
Autoencoder	0.1
Wavelet Transform	0.7
Hilbert Huang Transformation	1.2
Auto Regression Model	1.4

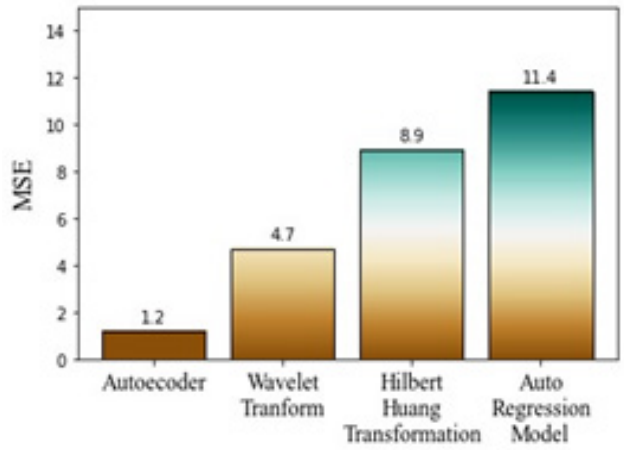


Figure 6. Comparison of MSE.

Wavelet Transform, Hilbert Huang Transformation, and Auto Regression model values are 0.7%, 1.2%, and 1.4% respectively. Table 3 provides BER values for different techniques, where the Autoencoder achieves the lowest BER value of 0.1, confirming its efficiency in reducing bit errors compared to other methods.

Table 4. MSE Values

Method	MSE Value
Autoencoder	1.2
Wavelet Transform	4.7
Hilbert Huang Transformation	8.9
Auto Regression Model	11.4

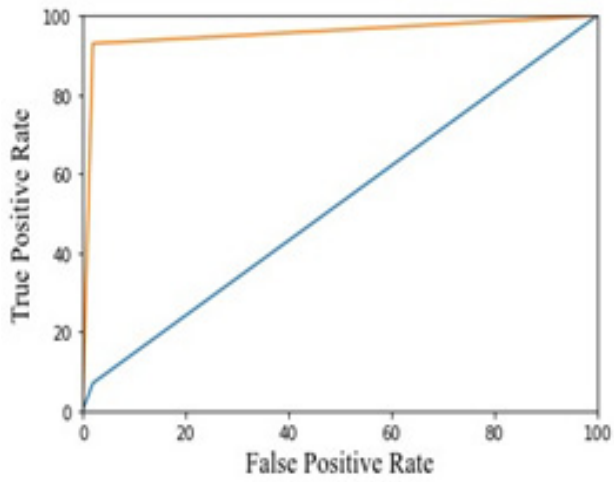


Figure 7. Analysis of ROC curve.

Table 4 lists the MSE values, highlighting that the Autoencoder method results in the lowest Mean Square Error (1.2), whereas the Auto Regression Model shows the highest error value (11.4). Figure 6 shows the comparison of MSE. The MSE (Mean Square Error) is a measure of the quality of an estimator. The proposed method of autoencoder error value is 1.2%, Wavelet Transform 4.7%, Hilbert Huang Transformation is 8.9 %, and Auto Regression model is 11.4% respectively. This demonstrates the proposed model has poorer MSE than the current approaches.

Table 5. ROC Metrices

Metric	Value (Approximate)
True Positive Rate (TPR)	~98-100 %
False Positive Rate (FPR)	~0-5 %
AUC (Area Under Curve)	Likely close to 1.0

The graph known as the ROC curve (Receiver Operating Characteristic) displays a classification model's performance across all categorization thresholds. Figure 7 shows in the upcoming section some existing approaches were taken for validating the proposed model performance. The existing model is taken as DBN (Deep Belief Network), RBF (Radial Basis Function) as well as Deep Neural Networks (DNN). Table 5 illustrates

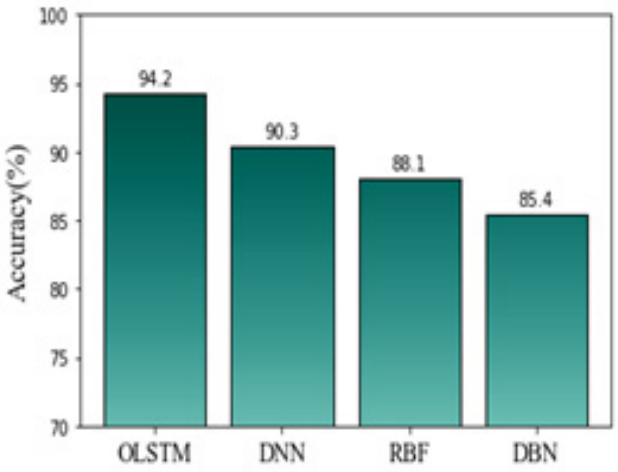


Figure 8. Accuracy comparison.

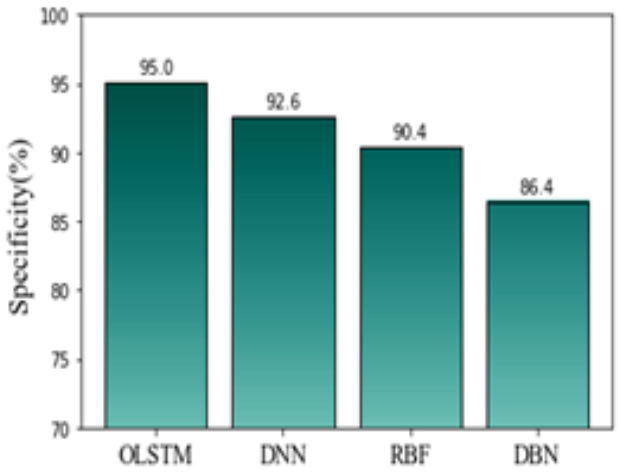


Figure 9. Comparison of specificity.

the ROC metrics, showcasing a high True Positive Rate (TPR) of approximately 98-100 % and a low False Positive Rate (FPR) of 0-5 %, indicating the strong classification performance of the model.

Table 6. Accuracy values

Method	Accuracy (%)
OLSTM	94.2
DNN	90.3
RBF	88.1
DBN	85.4

Table 7. Specificity Values

Method	Specificity (%)
OLSTM	95.0
DNN	92.6
RBF	90.4
DBN	86.4

The accuracy values that were determined using the confusion matrix are displayed in Figure 8. The accuracy of the suggested technique is 94.2%, whereas that of

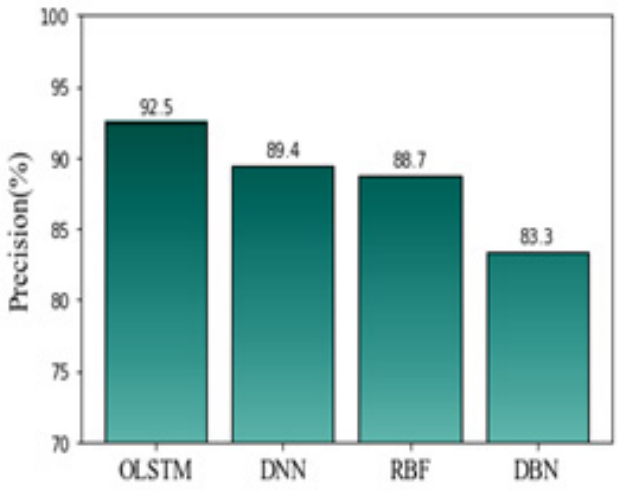


Figure 10. Comparison of precision.

DNN is 90.3%, RBF is 88.1%, and DBN is 85.4%. When compared to existing methods, the suggested model is more productive. A comparison between the suggested and present procedures is demonstrated in Figure 9. The fallout from the proposed technique is 95%, compared to 92.6% from the current DNN, 90.4% from RBF, and 86.4% from DBN. As a result, compared to standard models, the suggested model provides better results. Table 6 summarizes the accuracy values for various models, revealing that the OLSTM model achieves the highest accuracy of 94.2%, while DBN performs the lowest at 85.4%.

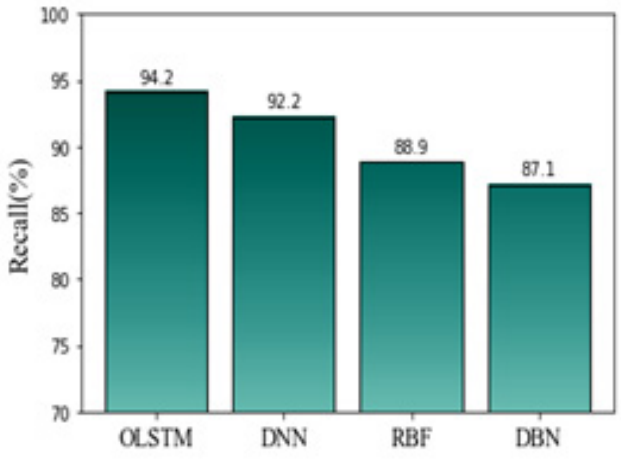


Figure 11. Comparison of recall.

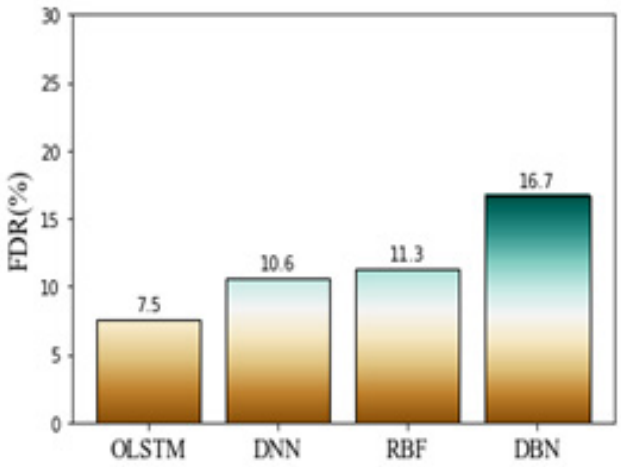


Figure 13. Comparison of FDR.

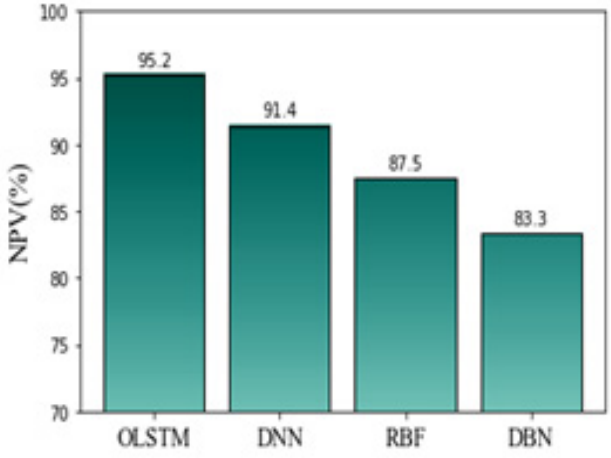


Figure 12. Comparison of NPV.

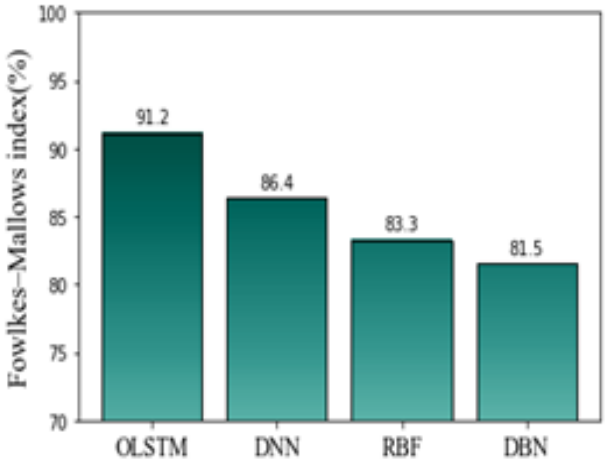


Figure 14. Comparison of fowlkes-mallows index.

Table 7 presents specificity values, where OLSTM achieves the best specificity score of 95.0%, confirming its ability to distinguish between fault and non-fault cases effectively.

The precision of the suggested and used approaches is in Figure 10. The precision of the proposed approach is 92.5%, while that of DNN, RBF, and DBN is 89.4%, 88.7%, and 83.3%, respectively. The comparison shows that the suggested approach outperforms conventional models in terms of precision. Figure 11 compares the recall of recommended and current techniques. Compared to other existing methods like DNN, RBF, and DBN, which have recall values of 92.2%, 88.9%, and 87.2%, the proposed OLSTM has a recall value of 94.2%.

Figure 12 compares the NPV of recommended and current techniques. The NPV of the suggested approach is 95.2%, while that of DNN, RBF, and DBN is 91.4%, 87.5%, and 83.3%, respectively. The comparison shows that the suggested approach outperforms conventional models in terms of NPV. The FDR of the proposed and suggested approaches is shown in Figure 13. The accuracy of the suggested technique is 7.5%, whereas that of DNN is 10.6%, RBF is 11.3%, and DBN is 16.7%. In contrast to existing techniques, the suggested model is more efficient

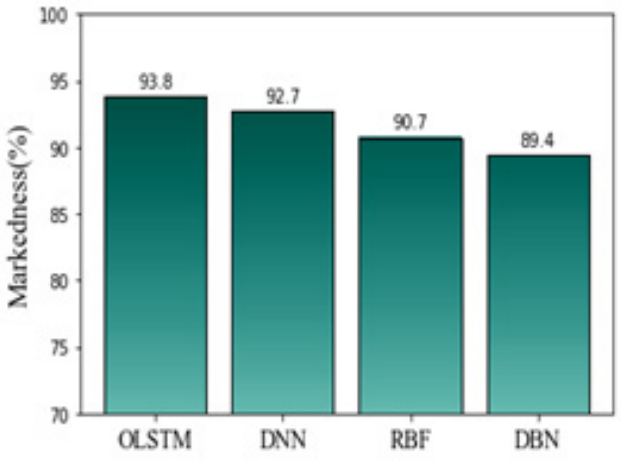


Figure 15. Markedness comparison.

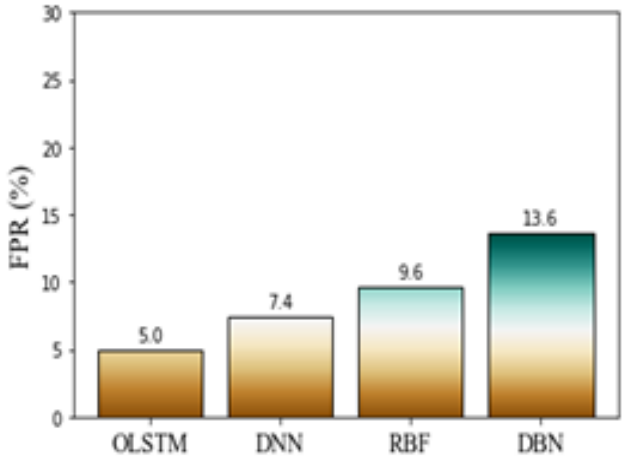


Figure 17. FPR comparison.

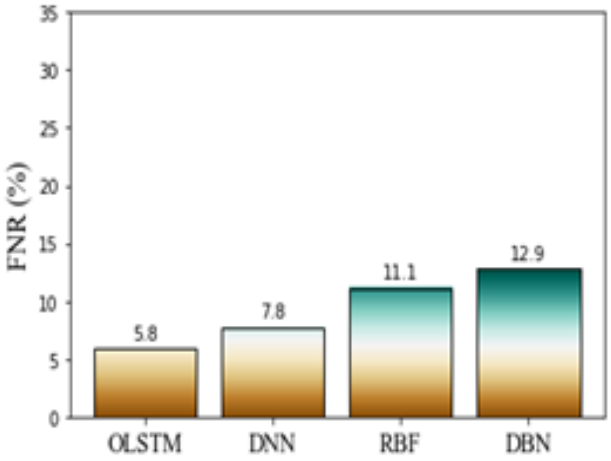


Figure 16. Comparison of FNR.

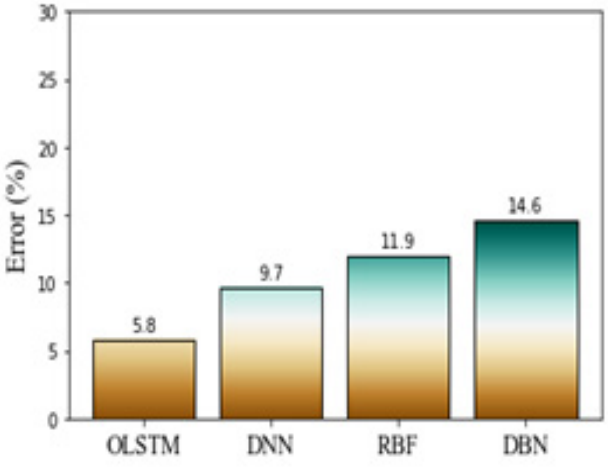


Figure 18. Comparison of error.

Figure 14 shows the Fowlkes-Mallows index's comparison. It shows the value of Fowlkes-Mallows index in the proposed OSTM is 91.2%, DBN is 81.5%, RBF is 83.3% and DNN is 86.4%. The proposed model outperforms conventional methodologies. Then the comparison of the suggested model and current model markedness is depicted in Figure 15. The proposed OSTM attains 93.8% Markedness, DBN attains 89.4% Markedness, RBF attains 90.7% Markedness and DNN attains 92.7% Markedness. The proposed model outperforms conventional methodologies.

Figure 16 depicts an evaluation of planned and present approaches to FNR. Contrasted with other existing techniques, like DNN, RBF, and DBN with corresponding precision values of 7.8%, 11.1%, and 12.9%, the proposed approach's precision value has been discovered to be 5.8%. Figure 17 shows the false positive rate contrast between the recommended and current approaches. The proposed technique has a false positive rate is 5%, the existing DNN has 7.4%, RBF has 9.6% and DBN has 13.6%.

Figure 18 depicts the error comparison between the suggested as well as existing techniques. The suggested approach has an error rate of 5.8% DNN is 9.7%, RBF is 11.9% and DBN is 14.6% It proves that the suggested model outperforms the traditional models in terms of error rates. The F1_score is a measurement of the

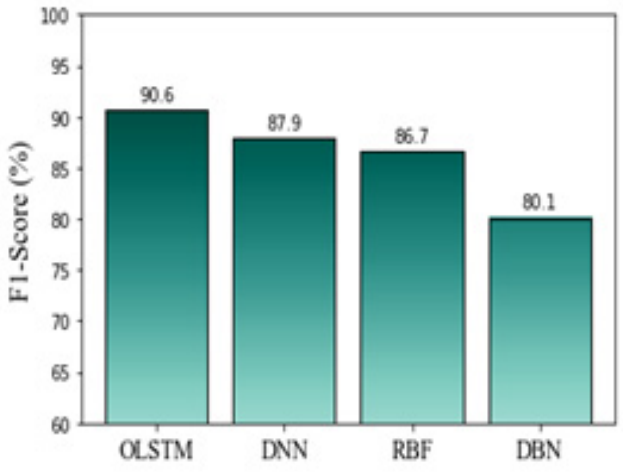


Figure 19. Comparison of F1-score.

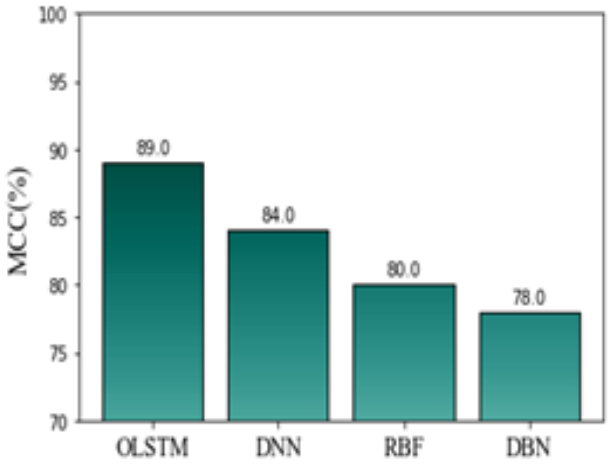


Figure 21. Comparison of MCC.

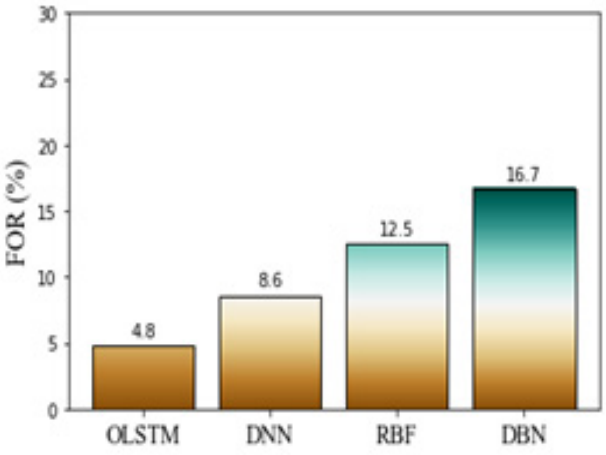


Figure 20. Comparison of FOR.

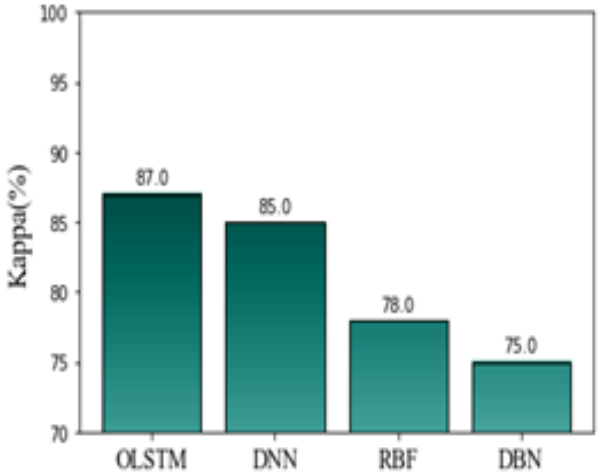


Figure 22. Comparison of Kappa.

harmonic mean of recall as well as precision, as seen in Figure 19. frequently employed as a multi-class and binary classification evaluation metric. Compared to other existing approaches, like DNN, RBF and DBN with corresponding F1_score values of 87.9%, 86.7%, and 80.1%, the recall value of the suggested approach was found to be 90.6%.

Figure 20 presents an evaluation of the suggested and existing methodologies for FOR. Compared to other methods now in use, such as DNN, RBF, and DBN with corresponding FOR values of 8.6%, 12.5%, and 16.7%, The FOR value of the suggested approach was found to be 4.8%. Figure 21 clearly shows the MCC of the proposed and existing comparison. The comparison shows the OLSTM has 89% MCC, DNN has 84% MCC, RBF has 80% MCC and DBN has 78% MCC.

The Kappa disparity between the suggested and current techniques is seen in Figure 22. The error rate of the suggested approach is 87%, DNN is 85%, RBF is 78% and DBN is 75%. It shows that the suggested model outperforms the traditional models in terms of kappa. As shown in Figure 23, the negative likelihood ratio is computed by separating the total number of components that truly belong to the quantity of actual positives in the positive class. Compared to other methods now in use, such as DNN, RBF, and DBN with corresponding negative

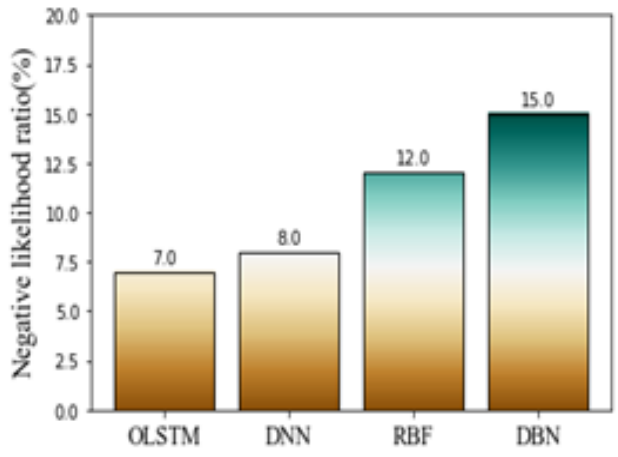


Figure 23. Comparison of negative likelihood ratio.

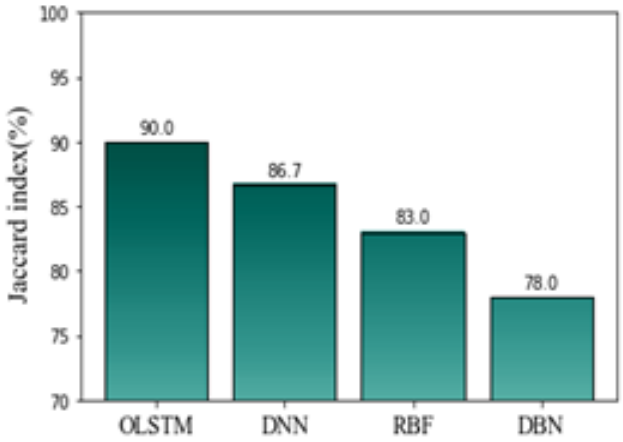


Figure 24. Jaccard index comparison.

likelihood ratio values of 8%, 12%, and 15%, it was found that the recall value of the suggested approach was 7%.

Figure 24 illustrates the Jaccard index comparison between the proposed and current approaches. The suggested approach's Jaccard index rate is 90%, DNN is 86.7%, RBF is 83% and DBN is 78%. It proves that the suggested model is more valuable than the traditional one. As shown in Figure 25, Informedness is computed and contrasted with existing models. Compared to other methods now in use, such as DNN, RBF, and DBN with matching recall values of 91%, 89%, and 85%, the proposed method's recall value was discovered to be 92%. This demonstrates that the proposed model produces superior results than the conventional methods.

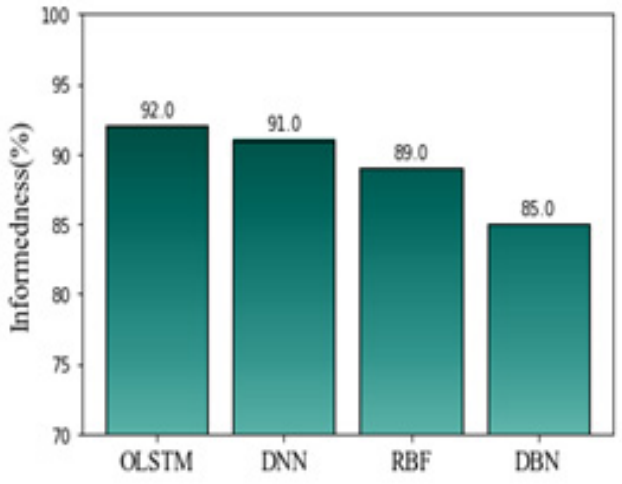


Figure 25. Comparison of informedness.

5.0 Conclusion

Novel optimized LSTM with autoencoder denoising is employed in the suggested model to detect faults effectively. Consequently, a standard source of information about mechanical vibration is collected in a signal form by using the sensor. Autoencoder denoising is one of the pre-processing techniques used to reduce vibration and noise. Finally, these pre-processed data were used to train and verify a successful OLSTM classifier for the identification of Mechanical vibration. The LSTM classifier performance is enhanced by using shell game optimization thus improving the accuracy of the proposed model. Performance metrics involving precision, accuracy, recall, as well as specificity are used to gauge the effectiveness of the suggested methodology, with values of 94.2%, 92.5%, 94.2%, and 95%, respectively. The drawback associated with this method is challenging to accurately ascertain the speed at the precise vibration and noise location. In the future, gather train bogie vibration features of the high-speed train as feasible and increase diagnostic accuracy, effective active control model-based deep learning model will be developed to enhance the prediction process.

6.0 References

1. Qobulov J, Barotov J. Effective organization of technologies for speeding up freight transportation in railway transport. E3S Web Conf. 2023; 389:05042. https://doi.org/10.1051/e3sconf/202338905042

2. Morihladko P, Dolinayová A. Increasing the efficiency of the transport of single wagon consignments- A tool for sustainable freight transport. Transport Technol. 2023; 19(2):13-17. https://doi.org/10.2478/ttt-2023-0009
3. Oladunni OJ, Mpofu K, Olanrewaju OA. Greenhouse gas emissions and its driving forces in the transport sector of South Africa. Energy Rep. 2022; 8:2052-61. https://doi.org/10.1016/j.egyr.2022.01.123
4. Nowell DA. Geology of Marseilles to Italy high-speed TGV railway line compared to HS2 in Britain. Geol Today. 2021; 37(1):23-30. https://doi.org/10.1111/gto.12338
5. Gu YW, Nie X, Yan AG, Zeng JH, Liu YF, Jiang YX. Experimental and numerical study on vibration and structure-borne noise of high-speed railway composite bridge. Appl Acoust. 2022; 192:108757. https://doi.org/10.1016/j.apacoust.2022.108757
6. Peng Y, Sheng X, Cheng G. Modelling track and ground vibrations for a slab ballastless track as an infinitely long periodic structure subject to a moving harmonic load. J Sound Vib. 2020; 489:115760. https://doi.org/10.1016/j.jsv.2020.115760
7. Karthick L, Michel J, Mallireddy N, Vadivukarasi L. Modelling and analysis of an EN8 crankshaft in comparison with AISI 4130 crankshaft material. Mater Today Proc. 2022; 52:1036-40. https://doi.org/10.1016/j.matpr.2021.10.484
8. Kane PV, Andhare AB. End of the assembly line gearbox fault inspection using artificial neural network and support vector machines. Int J Acoust Vib. 2019. https://doi.org/10.20855/ijav.2019.24.11258
9. Karthick L, Michel J, Jagadish CA. Vehicle safety system for two wheeler-A critical review. Mater Today Proc. 2022; 52:1594-7. https://doi.org/10.1016/j.matpr.2021.11.258
10. Karthick L, Sivakumar S, Sasikumar A, Prabhu A, Kumar JS, Vadivukarasi L. A comparison and analysis of mechanical properties of glass fiber and banana fiber composite. Mater Today Proc. 2022; 52:398-402. https://doi.org/10.1016/j.matpr.2021.09.073
11. Martínez-Llop PG, Bobi JDDS, Ortega MO. Time consideration in machine learning models for train comfort prediction using LSTM networks. Eng Appl Artif Intell. 2023; 123:106303. https://doi.org/10.1016/j.engappai.2023.106303
12. Isa NAM, Mamat WMFW. Clustered-hybrid multilayer perceptron network for pattern recognition application. Appl Soft Comput. 2011; 11(1):1457-66. https://doi.org/10.1016/j.asoc.2010.04.017
13. Cao Y, Xiang Q, Li B, Li Z. Field measurement and energy analysis of ground-borne vibration around high-speed railway viaduct. Shock Vib. 2023; 2023:4640726. https://doi.org/10.1155/2023/4640726
14. Karthick L, Mallireddy N, Yogaraja J, Sivakumar S, Sasikumar A. Modelling and analysis of an EN8 crankshaft material in comparison with forged steel crankshaft. Mater Today Proc. 2021; 47:6168-72. https://doi.org/10.1016/j.matpr.2021.05.079
15. Karthick L, Umashankar M, Singh AK, Bhambere VL, Xavier LF, Bhandari R. Mechanical and wear behavior of aluminium metal matrix composites reinforced ceramics materials for light structures. J Mines Metals Fuels. 2024; 1347-59. https://doi.org/10.18311/jmmf/2024/46077
16. Wu H, Wu P, Guo J, Zhou S, Wei J. Current signal characteristics analysis of transmission system in high-speed train under abnormal vibration conditions. Veh Syst Dyn. 2023; 61(4):1151-67. https://doi.org/10.1080/00423114.2022.2071745
17. Zhang C, Kordestani H, Shadabfar M. A combined review of vibration control strategies for high-speed trains and railway infrastructures: Challenges and solutions. J Low Freq Noise Vib Active Control. 2023; 42(1):272-91. https://doi.org/10.1177/14613484221128682
18. Qin N, Du J, Zhang Y, Huang D, Wu B. Fault diagnosis of multi-railway high-speed train bogies by improved federated learning. IEEE Trans Veh Technol. 2023; 72:7184-94. https://doi.org/10.1109/TVT.2023.3242433
19. Liu J, Xu K, Cai B, Guo Z. Fault prediction of on-board train control equipment using a CGAN-enhanced XGBoost method with unbalanced samples. Machines. 2023; 11(1):114. https://doi.org/10.3390/machines11010114
20. Sun H, He D, Lao Z, Jin Z, Liu C, Shan S. Fault diagnosis of train traction motor bearing based on improved deep residual network. Proc Inst Mech Eng Part C J Mech Eng Sci. 2024; 238(7):3084-99. https://doi.org/10.1177/09544062231196938
21. Dehghani M, Montazeri Z, Malik OP, Givi H, Guerrero JM. Shell game optimization: A novel game-based algorithm. Int J Intell Eng Syst. 2020; 13(3):246-55. https://doi.org/10.22266/ijies2020.0630.23
22. The vibration sensor on railway lines [dataset]. Available from: https://researchdata.up.ac.za/articles/dataset/The_vibration_sensor_on_railway_lines/24973911